the attenuation rate flattens out at larger depths of vegetation. This model is a reduction of eqn. 1 and is given by

$$A = -\left(A_m\left(1-\exp\left(-\frac{R_0 d}{A_m}\right)\right)\right) \qquad (2)$$

where A_m is the maximum attenuation, R_0 is the initial attenuation rate and d is the vegetation depth. Values obtained for this model using the measured data are shown in Table 2.

Table 2: MAR model parameter values from measured data

Model parameters	Fermi Avenue		The Mound at 5m	
	11.2GHz	20GHz	11.2GHz	20GHz
R_0 [dBm]	1.34	1.32	0.54	1.72
A_m [dB]	55.55	38.52	7.02	16.00

Graphs obtained using the two models and parameters listed above are superimposed on measured data in Figs. 1 – 4.

Conclusion: In Fig. 1, it can be seen that the NZG model gives a better fit than the MAR model. In Figs. 2 – 4, the two models give near identical fit. The NZG model is more suited for vegetation media of relatively small depths. There is a pronounced difference between the modelled results at 11.2GHz, shown in Fig. 1. This could be due to gaps caused by the absence of leaves and wind movement. More consistency is expected in the foliated state. The data has a mean variation of 8.5dB over all vegetation depths. This is believed to be the result of fluctuations in the wind and also because, especially in the case of the copse, the vegetation was not particularly dense. For 20GHz, a greater variation in the recorded signal strength at each vegetation depth is seen. This is expected owing to the smaller wavelength being able to propagate through smaller gaps in the vegetation. Ground reflections are believed to be responsible for normalised data attaining higher values than 0dB at some vegetation depths, in Fig. 3. Further work is needed to account for ground reflections, frequency dependency and the effects on measured data variation caused by fluctuations in wind speed and density of the vegetation material.

Acknowledgments: The authors wish to thank M.S. Ding for his assistance and members of RAL for their help and collaboration.

2 August 1995
Electronics Letters Online No: 19951215

R.B.L. Stephens and M.O. Al-Nuaimi (*Department of Electronics and Information Technology, University of Glamorgan, Pontypridd, CF37 1DL, United Kingdom*)

References

1 AL-NUAIMI, M.O., and HAMMOUDEH, A.M.: 'Measurements and predictions of attenuation and scatter of microwave signals by trees', *IEE Proc. Microw. Antennas Propag.*, 1994, **141**, (2)
2 SEVILLE, A., and CRAIG, K.H.: 'A semi-empirical model for millimetrewave vegetation attenuation rates', *Electron. Lett.*, 1995, **31**, (17), pp. 1507–1508
3 BACON, D.F.: Private communication, Radiocommunications Agency, December 1994

Performance gain of S-macrodiversity system in log-normal shadowed Rayleigh fading channel

Li-Chun Wang and Chin-Tau Lea

Indexing terms: Cochannel interference, Diversity reception, Fading Rayleigh channels

The authors offer an exact analysis for cochannel interference of a macrodiversity cellular system, called *S*-macrodiversity, where the branch selection is based on the local mean average signal power. In the past, most studies on macrodiversity have only included the shadowing effect. The authors' model includes both log-normal shadowing and Rayleigh fading.

Introduction: In a cellular system, the effects of the surrounding buildings, terrain and trees cause a large variation in signal strength received by a mobile unit. Analyses have shown that this variation degrades the system performance, and the resulting degradation is usually called the shadowing effect. We can achieve a more uniform coverage and reduce the shadowing effect by using two or more cites to serve a connection; the probability of two bad paths is obviously smaller than that of one. This technique, a large-scaled selection space diversity, is usually called macrodiversity.

The performance is usually represented in terms of cochannel interference (CCI) probability, which is defined as the probability that the desired signal level is less than the required receiver threshold due to excessive interference. Traditionally, three kinds of link measurement have been proposed:

(i) *S/I-macrodiversity:* The signal to interference ratio (S/I) is constantly computed and the branch with the largest S/I is selected, the signal of which is sent to the input of the receiver.

(ii) *S-macrodiversity:* The signal power (S) is constantly measured and the branch with the largest S is selected.

(iii) *(S + I)-macrodiversity:* The signal is mixed with interference; i.e. ($S + I$), is constantly measured and the branch with the largest ($S + I$) is selected.

Each technique requires a different degree of implementation complexity. For example, ($S + I$)-macrodiversity is the easiest to implement and only the received signal ($S + I$) is monitored. The S-macrodiversity, however, requires that the interference is separated from the received signal. Because S is usually much larger than I, the difference between S-macrodiversity and ($S + I$)-macrodiversity is small. The most desirable kind of link diversity, of course, is S/I-macrodiversity. However, a direct measurement of S/I is usually not obtainable.

In this Letter, we analyse the performance gain of S-macrodiversity. One reason we choose S-macrodiversity is that it is a close approximation to the ($S + I$)-macrodiversity, which is easy to implement. The other reason is that we can find an exact analysis for this case with fading. In the past, most analysis on macrodiversity is for shadowing only [1, 2]. In our model for S-macrodiversity, we can easily include Rayleigh fading and compare the performance difference between the models with and without fading. The signal we propose to measure is the slow-varying local means, instead of the instantaneous signal power. If the latter is used, the fast varying nature of the instantaneous signal power can make the mobile unit switch basestation constantly, which is certainly undesirable. Furthermore, the local mean, which is a result of shadowing only, has a higher correlation between the forward link and reverse link than the instantaneous signal power, which is a result of both shadowing and fading effects. Thus the offered uplink analysis can also be seen as an approximation on the downlink performance even though they are not exactly the same.

Pure shadowing channel: In [1, 2], the CCI probability of the S-macrodiversity cellular system in the pure shadowing channel is expressed as

$$\begin{aligned} F_S(\lambda_{th}) &= Prob(max(S_1, S_2, \cdots, S_L)/I \le \lambda_{th}) \\ &= 1 - L\int_0^\infty \left[\int_{-\infty}^{\frac{x}{\lambda_{th}}} \frac{1}{\sqrt{2\pi}\sigma_I y}\exp\left[\frac{-(\ln y - \ln \Upsilon_I)^2}{2\sigma_I^2}\right]dy\right] \\ &\times\left[1-Q\left(\frac{\ln x - \ln \Upsilon_k}{\sigma_k}\right)\right]^{L-1}\frac{1}{\sqrt{2\pi}\sigma_k x}\exp\left[\frac{-(\ln x - \ln \Upsilon_k)^2}{2\sigma_k^2}\right]dx \end{aligned} \qquad (1)$$

where

$$Q(x) = \int_x^\infty \frac{1}{\sqrt{2\pi}}\exp(-x^2/2)dx$$

σ_k is the shadowing spread and Υ_k is the area mean power of the desired signal in the kth branch. Furthermore, the sum of multiple log-normal interfering signals I is characterised by another log-normal random variable with variance σ_I and area mean Υ_I by using the approach in [3].

Shadowed Rayleigh fading channel: Let Z be the best local mean of the desired signal among the L diversity branches, i.e.

$$Z = max(\Omega_1, \Omega_2, \cdots, \Omega_L) \tag{2}$$

where Ω_k is the log-normal distributed local mean of the signal power from the kth branch. If each branch is mutually independent and identically distributed (IID), the probability density function (PDF) of Z is

$$f_Z(x) = L\left[1 - Q\left(\frac{\ln x - \ln \Upsilon_k}{\sigma_k}\right)\right]^{L-1} \times \frac{1}{\sqrt{2\pi}\sigma_k x} \exp\left[\frac{-(\ln x - \ln \Upsilon_k)^2}{2\sigma_k^2}\right] \tag{3}$$

For a given local mean Z, the PDF of the desired signal power y_d under the shadowed Rayleigh fading channel is exponentially distributed, i.e.

$$f_{y_d}(y_d \mid Z) = \frac{1}{Z} \exp\left[-\frac{y_d}{Z}\right] \tag{4}$$

In [4], the exact formula of the conditional CCI probability given the local mean of the desired signal is derived under the shadowed Rayleigh fading channel. We extend the results in [4] to the macrodiversity cellular system. More specifically, the local mean of the desired signal in [4] is now replaced by the best local mean selected from among the L base stations, denoted by Z, of which the PDF is given in eqn. 3. We assume that the log-normal distributed local means of the n interfering signals ω_i, $i = 1, ..., n$, are IID random variables; then the conditional CCI probability given Z and n can be obtained by using the similar procedures in [4] as follows:

$$Prob(y_d \le \lambda_{th} \mid Z, n) = 1 - \prod_{i=1}^{n} \int_0^{\infty} \frac{Z}{\sqrt{2\pi}(Z + \lambda_{th}\omega_i)\sigma_i\omega_i} \times \exp\left[\frac{-(\ln \omega_i - \ln \Upsilon_i)^2}{2\sigma_i^2}\right] d\omega_i \tag{5}$$

where ω_i is the log-normal distributed local mean of the ith interferer with shadow spread σ_i and area mean Υ_i, $i = 1, ..., n$ and λ_{th} is the threshold required at the receiver. Averaging over Z in eqn. 5, we obtain

$$\begin{aligned} &Prob(y_d \le \lambda_{th} \mid n) \\ &= 1 - \int_0^{\infty} L\left[1 - Q\left(\frac{\ln Z - \ln \Upsilon_k}{\sigma_k}\right)\right]^{L-1} \\ &\quad \times \frac{1}{\sqrt{2\pi}\sigma_k Z} \exp\left[\frac{-(\ln Z - \ln \Upsilon_k)^2}{2\sigma_k^2}\right] \\ &\quad \times \left[\prod_{i=1}^{n} \int_0^{\infty} \frac{Z}{\sqrt{2\pi}(Z + \lambda_{th}\omega_i)\sigma_i\omega_i} \exp\left[\frac{-(\ln \omega_i - \ln \Upsilon_i)^2}{2\sigma_i^2}\right] d\omega_i\right] dZ \end{aligned} \tag{6}$$

By letting $\alpha = \ln(Z/\Upsilon_k)/(\sqrt{2}\sigma_k)$ and $\beta = \ln(\omega_i/\Upsilon_i)/(\sqrt{2}\sigma_i)$, we can transform eqn. 6 into a Hermite integration form and apply the Hermite polynomial approach to obtain the numerical result as follows:

$$\begin{aligned} Prob(y_d \le \lambda_{th} \mid n) &= 1 - \int_{-\infty}^{\infty} f(\alpha) \exp(-\alpha^2) d\alpha \\ &\simeq 1 - \sum_{l=1}^{l=m} f(x_l)\phi_l \end{aligned} \tag{7}$$

where

$$f(x_l) = \frac{L}{\pi}\left[1 - Q\left(\sqrt{2}x_l\right)\right]^{L-1} \times \left[\prod_{i=1}^{n} \sum_{h=1}^{m} \frac{\Upsilon_k \exp\left(\sqrt{2}\sigma_k x_l\right) \phi_h}{\left(\Upsilon_k \exp\left(\sqrt{2}x_l\sigma_k\right) + \lambda_{th}\Upsilon_i \exp\left(\sqrt{2}\sigma_i x_h\right)\right)}\right] \tag{8}$$

where ϕ_l and ϕ_h are the weight factors, x_l and x_h are the roots of the mth order Hermite polynomial, respectively, Υ_k and Υ_j are the area means of the desired signal and interfering signal, respectively, and σ_k and σ_j are the shadow spread of the desired signal and interfering signal, respectively.

Table 1: S-macrodiversity gain (DG) and received signal to interference ratio (S/I) in terms of 5 and 10% cochannel interference probability (CCIP) in pure shadowing channel and shadowed Rayleigh fading channel

L	Pure shadowing				Shadowing & Rayleigh fading			
	5% CCIP		10% CCIP		5% CCIP		10% CCIP	
	S/I	DG	S/I	DG	S/I	DG	S/I	DG
	dB	dB	dB	dB	dB	dB	dB	dB
1	10.96	–	13.69		5.49	–	9.55	–
2	15.78	4.82	18.12	4.43	9.78	4.29	13.54	3.99
3	17.97	7.01	20.46	6.77	11.78	6.29	15.51	5.96
4	19.41	8.45	21.80	8.11	13.13	7.64	16.80	7.25

a

L	Pure shadowing				Shadowing & Rayleigh fading			
	5% CCIP		10% CCIP		5% CCIP		10% CCIP	
	S/I	DG	S/I	DG	S/I	DG	S/I	DG
	dB	dB	dB	dB	dB	dB	dB	dB
1	0.64	–	5.11	–	-3.09	–	2.28	–
2	8.54	7.9	12.52	7.41	4.27	7.36	9.28	6.96
3	12.22	11.58	16.06	10.95	8.00	11.09	12.62	10.34
4	14.36	13.72	18.39	13.28	10.23	13.33	15.11	12.83

b

a $\sigma_k = \sigma_i = 6$dB

b $\sigma_k = \sigma 6.5\,\pi\tau = 10$dB

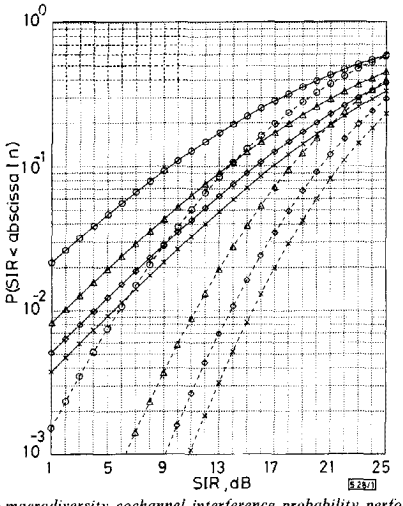

Fig. 1 *S-macrodiversity cochannel interference probability performance in pure shadowing channel and shadowed Rayleigh channel*

$n = 2$, $\sigma_k = \sigma_i = 6$dB, $a = b = 2$, $g = 0.15R$ and $R_u = 5.3R$, where R is cell radius, and R_u is distance between receiver and interferers
- - - - pure shadowing channel
——— shadowed Rayleigh channel
—○— no diversity
—△— two-branch diversity
—◇— three-branch diversity
—×— four-branch diversity

Numerical results and discussions: Consider a dual slope path loss model $p_r/p_t = 1/d^a(1 + g/d)^b$, where p_r/p_t is the ratio of received power to the transmitted power, d is the distance, $a = b = 2$ and $g = 0.15$ times the cell radius in our case. Let the mobile be at the cell boundary R and the interferers be 5.3 R away. Fig. 1 shows the performance of an S-macrodiversity cellular system in a pure shadowing channel and in a shadowed Rayleigh fading, respectively. It is shown that with three-branch macrodiversity in an environment with 6dB shadowing spread, the 90 percentile S/I is

higher than 15.51dB in a shadowed Rayleigh fading channel and 20.46dB in a pure shadowing channel. This performance difference results from the fact that the *S*-macrodiversity system is suitable for measuring the slow-varying local mean power, instead of the fast-varying instantaneous signal power. Hence, the fast-varying Rayleigh fading components, embedded in the best local mean power signal among the selected diversity branches, may impose randomness and degrade the performance. For the 10% CCI probability in the case considered, the performance difference between the cases with and without Rayleigh fading is 4 – 5dB for diversity branches from 1 to 4. Table 1 lists the diversity gain (DG) and *S/I* performance for 5 and 10% CCI probability in the cases with 6 and 10dB shadow spreads, respectively. The diversity gain is defined as the *S/I* performance improvement compared to the case without diversity. For example, for $L = 1$ and CCIP=10%, Table 1*a* reads that *S/I* = 13.69 and 9.55. This means that with 90% probability, the *S/I* will be > 13.69 and 9.55dB for cases with and without fading, respectively. Even with fading, we still see that conventional conclusions about diversity gain still hold even after fading is added, such as (i) higher shadow spread leads to the higher diversity gain and (ii) the diversity gain per branch decreases as the diversity branch is increased. More interesting, we observe that the diversity gain seems to be little affected by including fading in the model.

15 August 1995
Electronics Letters Online No: 19951209

Li-Chun Wang and Chin-Tau Lea (*Georgia Institute of Technology, School of Electrical and Computer Engineering, Atlanta, GA 30332-0250, USA*)

References

1 WANG, L.C., and LEA, C.T.: 'Macrodiversity co-channel interference analysis', *Electron. Lett.*, 1995, **31**, (6), pp. 614–616
2 YEH, Y.H., WILSON, J.C., and SCHWARTZ, S.C.: 'Outage probability in mobile telephone with directive antennas and macrodiversity', *IEEE J. Sel. Areas Commun.*, 1984, **SAC-2**, pp. 507–511
3 SCHWARTZ, S.C., and YEH, Y.H.: 'On the distribution function and moments of power sums with log-normal components', *Bell Syst. Tech. J.*, 1982, **61**, pp. 1441–1462
4 LINNARTZ, J.-P.M.G.: 'Exact analysis of the outage probability in multiple-user mobile radio', *IEEE Trans.*, 1992, **COM-40**, pp. 20–23

VHF field strength measurements in Senegal

K.A. Hughes, F. Postogna and S.M. Radicella

Indexing terms: Radiowave propagation, Atmospheric EM wave propagation

Field strength measurements at a frequency of 215MHz were made for over two years on a 237km path in Senegal The results indicate field strength levels significantly in excess of those predicted, and with considerable seasonal and diurnal variability.

Introduction: With the aim of improving knowledge of radiowave propagation characteristics in tropical regions, an experiment was established in Senegal to acquire field strength measurement statistics at a frequency in the VHF band. Such statistics are essential for effective frequency planning and are particularly required for tropical regions for which propagation information is often lacking. Propagation in these regions is frequently prone to atmospheric super-refractivity and ducting, which are the mechanisms associated with high level signals likely to cause cochannel interference.

Path and equipment details: The signal level from the TV transmitter in Ziguinchor (southern Senegal) was received at Bambey (~140km east of Dakar) with an antenna 10m above local ground. The frequency was 215MHz, the ERP was 10kW and the effective antenna height was 200m. The propagation path, of length 237 km, was essentially flat with no significant terrain obstacles; the average distance of the path from the coast was ~50km. 1min values of signal level were recorded with a data logger and subsequently converted to field strength. The transmission schedule meant that the data corresponded essentially to the periods 1600 – 2400h on weekdays, and 1200 – 2400h at weekends and national holidays. The experiment ran for some 30 months (December 1992 – May 1995) and, with equipment failures, data were obtained on 66% of the days.

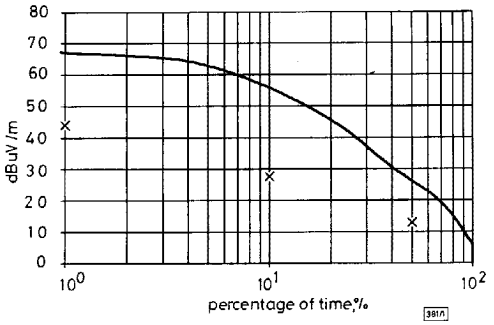

Fig. 1 *Cumulative frequency distribution for entire database of measurements and comparison with ITU-R predictions (X)*

Free-space field strength level estimated as 69.5dBμV/m
——— cumulative frequency distribution for entire database of measurements
× ITU-R predictions

Cumulative distribution of received field strength for entire measurement period: Fig. 1 shows the value of field strength (dBμV/m) exceeded against the percentage of measurement time for the entire database. The results are compared with predictions using internationally agreed methods of the ITU-R [1, 2]. Such methods generally provide long-term (e.g. annual) predictions and take little or no account of short-term (e.g. monthly) variability. For the region of west Africa containing Senegal, the appropriate propagation curves from these two methods are identical and correspond to those for a warm maritime region. Fig. 1 shows the predicted values at 50, 10 and 1% of the time. The results indicate serious discrepancies between predictions and measurements, in turn demonstrating that the level of super-refractivity in the region is far greater than previously estimated.

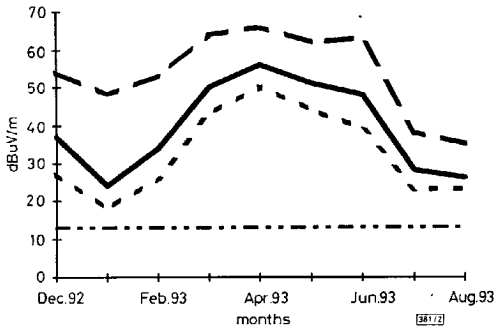

Fig. 2 *Monthly variation of field strength at three time percentages*

——— 50% of time
– – – – 10% of time
····· 70% of time
–·–·–· 50% of time (predicted)

Monthly variation: Cumulative distributions for each month reveal two interesting results. Firstly, comparisons with predictions show that, in many cases, the predictions are seriously underestimated.